Power Compensation Method for Coil Parameters Variation in LCC-S Wireless Power Transfer

Yuki Ouchi
Faculty of Science and Technology
Tokyo University of Science
Noda, Japan
ouchi.yuki21@gmail.com

Ryo Matsumoto
Graduate School of Frontier Sciences,
The University of Tokyo
Kashiwa, Japan

Takehiro Imura
Faculty of Science and Technology
Tokyo University of Science
Noda, Japan

Yoichi Hori
Faculty of Science and Technology
Tokyo University of Science
Noda, Japan

***Abstract*— Coil parameters variation due to manufacturing error or environment causes received power and efficiency decrease in wireless power transfer(WPT). Especially, self-inductance variation causes resonance misalignment, and the system can't maintain ideal characteristics including nominal received power. This paper proposes a power compensation method that controls only the receiving (Rx) side when coil parameters change. By using LCC circuit on the transmitter (Tx) side, wireless communication and power fluctuation due to coil parameter change on the Tx side are eliminated. On the Rx side, the received power is controlled by a DC/DC converter while the resonance misalignment is compensated by a branched capacitor. The proposed method can control the power and compensate the resonance misalignment concurrently. MATLAB Simulink simulation and experimental steady-state measurement results show that power compensation with varying capacitors on the Rx side can improve efficiency by compensating for resonance misalignment.**

Keywords—Wireless Power Transfer(WPT), LCC-S circuit, Detuning, Resonance misalignment ,DC/DC converter

I. INTRODUCTION

Wireless power transfer (WPT) has attracted attention[1],[2] as an effective way for charging electrical devices, such as electric vehicle (EVs) charging[3],[4], implantable medical devices[5],[6] and new space station[7].

This technology uses compensation capacitors on the transmitter (Tx) and receiver (Rx) sides, respectively[8], to adjust the resonance frequency, thereby enhancing transmission characteristics. In WPT, an S-S circuit with compensation capacitors inserted in series with the Tx-Rx coils are commonly used. However, the performance of WPT depends on the self-inductance and mutual inductance of the Tx and Rx coils. The self-inductance and mutual inductance of Tx and Rx coils change from their nominal values caused by manufacturing errors, aging and changes in the distance between coils from the design value[9]. Changes in mutual inductance and self-inductance cause power instability. For power compensation, several solutions are given in [10]-[13]. In [10], power compensation was achieved by varying the inverter drive frequency. In [11]-[13], power stabilization techniques were proposed by varying the equivalent resistance connected to the output part of the WPT circuit.

However, these cannot obtain ideal characteristics due to resonance misalignment caused by self-inductance changes. When resonance misalignment occurs at Tx and Rx side, transmission characteristics deteriorate[14]-[16]. Methods to improve the deterioration of transmission characteristics due to resonance misalignment include [17]-[22]. In [17], wireless communication is used between Tx and Rx side to correct resonance misalignment. However, the use of wireless communication is unsuitable due to the inevitable complexity of the system. In [18], spread spectrum is used by varying the frequency on the Tx side. A sensor coil is added on the Rx side and the phase difference on the Tx and Rx side is estimated. However, the coupling coefficients of the Rx coil and the sensor coil are assumed to be known, and if the coupling coefficients of the Rx coil and the sensor coil deviate, errors occur in the estimation. In [19], [20], systems were proposed that use PWM capacitors in the S-S circuit on the Tx and Rx sides and no other components or wireless communication beside PWM capacitors. However, to simplify the system, only the Rx side is preferred as the control point. In [21], A system was proposed that eliminates the need for communication and resonance mismatch compensation on the Tx side and compensates for capacitance on the Rx side. In [22], a resonance misalignment compensation method was proposed for the Rx side only, using an LCC circuit on the Tx side. However, it is not possible to control the resonance misalignment concurrently with the power, because the maximum value of the power is tracked to compensate for the change in self-inductance.

This paper proposes a method of resonance misalignment compensation in which the value of the load can be varied. In the proposed method, the input impedance is varied by controlling the duty ratio of the DC/DC converter, which equivalently changes the resistance of the load at the output of the WPT to control the power. Compensation is performed to compensate for resonance misalignment without using wireless communication, maximizing efficiency by controlling only the Rx side.

II. RESONANT COMPENSATION SCHEME INDEPENDENT LOAD

To simplify the analysis, a fundamental approximation is applied and the equivalent series resistance(ESR) of each inductor and capacitor in the circuit is ignored. A simplified LCC-S circuit is shown in Fig. 1. In Fig. 1, L_1, L_2represent the self-inductance of the Tx and Rx coils and M represents the mutual inductance.

At resonance, in the LCC-S circuit, the following resonance condition (1), holds for the frequency ω_0 of the power supply and each element.

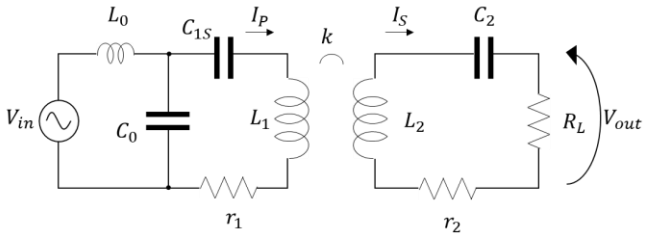

Fig. 1 Simplified circuit model of LCC-S components.

TABLE I : BASIC PARAMETER.

Symbol	Value
Operating Frequency of Inverter(f_0)	85 kHz
Input DC Voltage (E)	20 V
Compensation Inductor (L_0)	21 µH
Compensation Capacitor (C_0)	166 nF
Tx coil Resistance (r_1)	0.1 Ω
Rx coil Resistance (r_2)	0.1 Ω
Tx coil Inductance (L_1)	99.4 µH
Rx coil Inductance (L_2)	97.9 µH
Primary Capacitor (C_{1S})	39.5 nF
Mutual inductance (M)	20.5 µH
Resistance of Load (R_L)	3 Ω

$$\omega_0 = \frac{1}{\sqrt{L_0 C_0}} = \sqrt{\frac{C_0 + C_{1S}}{L_1 C_0 C_{1S}}} = \frac{1}{\sqrt{L_2 C_2}} \tag{1}$$

From (1), ac output power P_{out} on the Rx side is expressed as in (2).

$$P_{out} = \frac{M^2}{L_0^2 R_L} V_{in}^2 \tag{2}$$

(2) show that M^2 and P_{out} are proportional. This indicates that if M between Tx and Rx changes, the output power P_{out} cannot be maintained. Therefore, control is required to retain the power to the desired value. However, from (2), R_L also varies with P_{out}, so it is possible to compensate by changing R_L when M change occurs.

A. Robustness of resonance misalignment on Tx side

It has been reported that by keeping the current I_P in the Tx coil constant, P_{out} does not change when resonance shift caused by a change in L_1 occurs, even without any compensation for resonance shift by C_{1S} [21], [22].

As a method to keep the current flowing in the Tx coils constant, this paper uses an LCC circuit on the Tx side as in [22]. This eliminates the effect of resonance misalignment on the Tx side without using any control. Fig. 3 shows the result of a color map visualizing the relationship between the output power by taking the changes in C_{1S} and C_2 as axes, based on the parameters of TABLE I. The results show that P_{out} does not change when C_{1S} changes. However, it also shows that

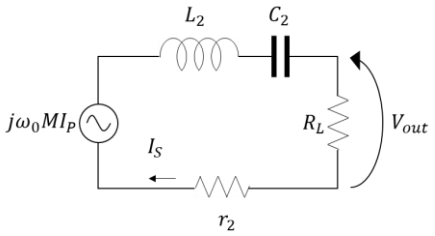

Fig. 2 Equivalent circuit of Rx Side.

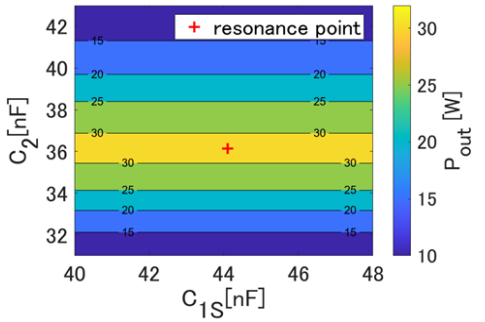

Fig. 3 Relationship between C_{1S}, C_2 and P_{out}. ($R_L = 6\ \Omega$)

the output power decreases with a change in C_2, indicating that the resonance misalignment needs to be corrected.

B. Proposed resonance compensation method

Rx side of the LCC-S circuit is shown in Fig. 2, with the residual impedance due to resonance misalignment on the Rx side being Z_2, as in equation (3).

$$Z_2 = \omega_0 L_2 - \frac{1}{\omega_0 C_2} \tag{3}$$

The current I_P flowing into the Tx coil is constant regardless of the effect of resonance shift on the Rx side and there is no interference on the Rx side, making wireless communication unnecessary. In static state, M is constant during resonance compensation, so the induced EMF (Electromotive Force) on the Rx side is constant.

The voltage of the load V_{out} is expressed as in (4).

$$|V_{out}| = \left| \frac{\omega_0 M R_L}{R_L + jZ_2} I_P \right| \tag{4}$$

When the resonance misalignment is corrected and $Z_2 = 0$, (4) coincides with the induced EMF and is independent of the size of the load.

Also, V_{out} takes the maximum value. From the above, this paper proposes that load-independent compensation of resonance misalignment is possible by varying the capacitor

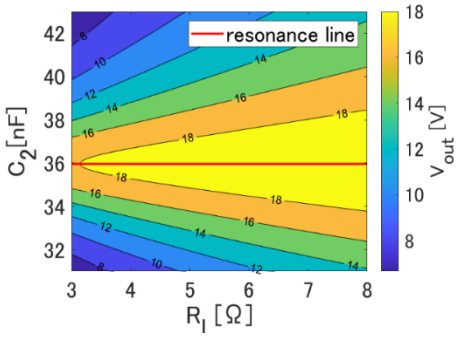

Fig. 4 Colormap of v_{out} as a function R_L and Z_2.

C_2 on the Rx side and searching for the maximum value of the output voltage V_{out}. The same conclusion can be obtained by a graphical approach. Fig. 4 shows a color map of the output voltage as a function of load R_L and reactance Z_2, based on the parameters of TABLE I. The closer to blue, the lower the voltage, and the closer to yellow, the higher the voltage. The red line corresponds to $Z_2 = 0$, indicating that the Rx side is in resonance. The voltage V_{out} is maximum, irrespective of the load value. The reason why the contour lines in Fig. 4 are not perfectly parallel to the horizontal axis is that the effect of resonance shift becomes smaller as the load R_L becomes larger.

Equivalently, the value of the load can be controlled by varying the duty ratio of the DC/DC converter in the LCC-S circuit as in [11]-[13]. In this paper, as in [11], [13], a buck converter is used to control the power consumed by the load by varying the duty ratio.

III. OVERVIEW OF THE SYSTEM

A. Overview of Proposed System

Fig. 5 shows the proposed system. The inverter on the Tx side delivers high frequency current to the LCC circuit. The power received by the S-circuit on the Rx side is converted by the buck converter after the bridge rectifier and consumed by the load. The PI controller aims to control power on the Rx side. The capacitors on the Rx side perform Maximum Point Tracking control (MPT) and compensate for resonance misalignments. To eliminate the effects of transients caused by the switching of branched capacitors, the control for compensation of resonance misalignment is sufficiently slower than the constant power control.

B. Control Scheme of Branched Capacitor

In this paper, the branched capacitor is created as shown in Fig. 6. The capacitor C_{2b} is attached at the bottom. On top of it, the total capacitance C_2 is varied by attaching parallel capacitors $\Delta C_2, 2\Delta C_2, 4\Delta C_2, 8\Delta C_2$ and $16\Delta C_2$, which can be connected or disconnected by switches.

IV. SIMULATION AND EXPERIMENT VERIFICATION

A. Simulation Verification

Theoretical verification was performed by simulation using MATLAB Simulink. The parameters are shown in TABLE I and TABLE II.

Assume that the inductance of the coils of Tx and Rx are shifted by 10%. On the Rx side, the resonance misalignment compensation starts at 31.5 nF and the capacitance is varied by 0.25 nF.

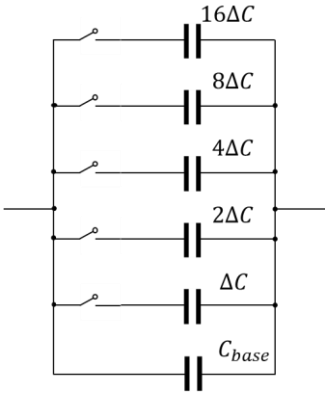

Fig. 6 Overview of branched capacitor.

TABLE II : SIMULATION PARAMETER.

Symbol	Value
Regulated Power (P_{ref})	20 W
Minimum Capacitance C_{2b}	31.5 nF
Increment Capacitance ΔC_2	0.25 nF
Control Frequency of Branched Capacitor f_c	100 Hz
Control Frequency of DC/DC Converter f_{dc}	100 kHz

Fig. 7 shows the results of the proposed method, where the right side of the dotted line indicates the area with constant power control. The trajectory of output power P_{out} is shown in Fig. 7 (a). Fig. 7 (b) shows the trajectory of branched capacitor C_2 on the Rx side with the red line indicating perfect resonance. In Fig. 7 (c), the trajectory of output voltage v_{out} is shown. The results show that the resonance misalignment compensation can be performed even when power control is performed as the resonance approaches. v_{out} increased rapidly because the duty cycle of the DC/DC converter decreased and the corresponding point in Fig. 4 shifted in the direction of increasing R_L. The simulation results show that the proposed control method can correct the resonance misalignment while controlling the power.

B. Experimental Verification

Next, an experimental validation was conducted. Fig. 8 shows the experimental view. The parameters of the experiment are shown in TABLE I and TABLE III. The produced branched capacitor has characteristics like TABLE IV.

The size of the Tx and Rx coils was 250 mm × 250 mm, the MOSFETs of the H-Bridge inverter and the DC/DC converter were BSM120D12P2C005, and the controller was

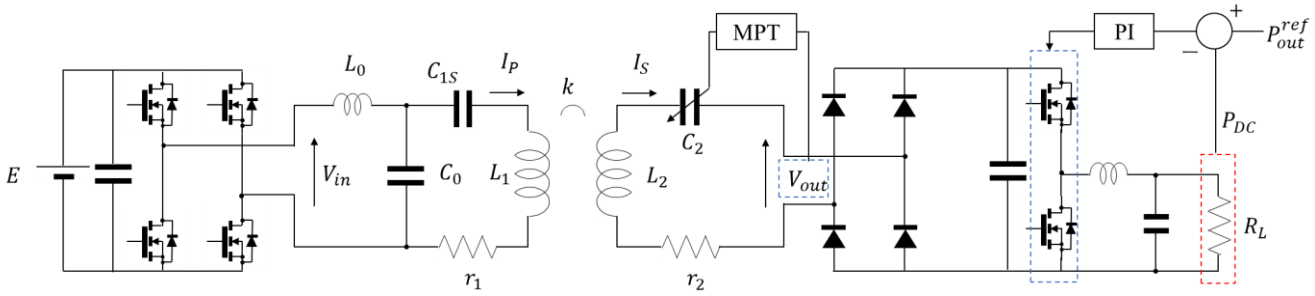

Fig. 5 Overview of control scheme of proposed method.

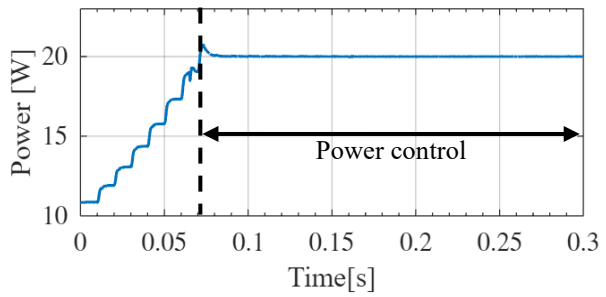

(a)

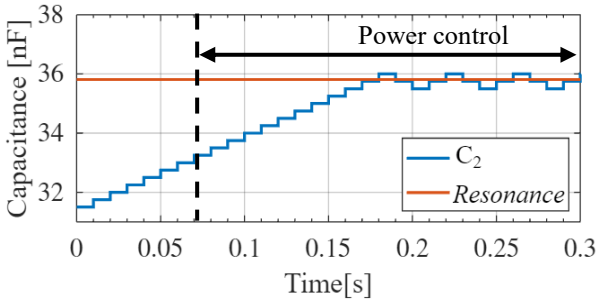

(b)

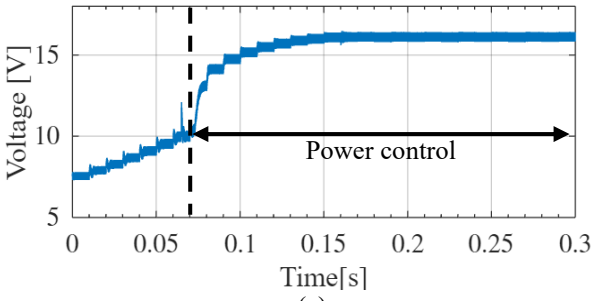

(c)

Fig. 7 Simulation results of the trajectory under applying proposed control scheme. (a) DC/DC converter output power. (b) capacitance. (c) output AC voltage.

PE-Expert4 from MyWay corporation. The capacitance was varied by 1 nF by switching connections manually. The duty ratio of the DC/DC converter was varied so that the output power P_{DC} of the buck converter was 15 W for each capacitance. When the effect of resonance misalignment was large and the power was less than 15 W, the duty ratio of the DC/DC converter was fixed at 0.95. TELEDYNE LECROY WaveSurfer 3000z oscilloscope was used as the measuring instrument to measure the RMS value of the output voltage of the LCC-S circuit, the phase difference between the current in the Tx coil and the current in the Rx coil, the AC/AC efficiency η, and the power consumed by the load, P_{DC}.

The results are shown in Fig. 9. The blue area in Fig. 9 shows where constant power control is not performed, and the duty ratio of the DC/DC converter is fixed at 0.95. From Fig. 9(a), the power is controlled to keep the power applied to the load at 15 W in the range of 34 nF to 39 nF.

Fig. 9(b) shows the phase difference between the current flowing in the Tx coil and the current flowing in the Rx coil when the capacitance is varied. Fig. 9(b) shows that the system is closest to resonance when the capacitance is 36 nF. Fig. 9(c) shows the relationship between each capacitance and the output voltage of the LCC-S circuit. Fig. 9 (c) shows

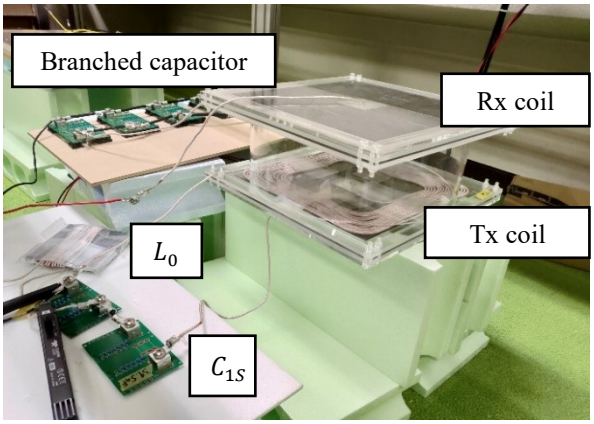

Fig. 8 Experiment setup.

TABLE III：EXPERIMENTAL PARAMETER.

Symbol	Value
Regulated Power (P_{ref})	15 W
Minimum Capacitance (C_{2b})	31 nF
Increment Capacitance (ΔC_2)	1 nF
Control Frequency of DC/DC Converter (f_{dc})	10 kHz

TABLE IV：BRANCHED CAPACITOR SPECIFICATION.

Symbol		Value
C_{base}	Capacitance [nF]	31.1
	Resistance[Ω]	0.41
ΔC	Capacitance [nF]	0.5
	Resistance[Ω]	1.13
$2\Delta C$	Capacitance [nF]	1.0
	Resistance[Ω]	0.27
$4\Delta C$	Capacitance [nF]	2.0
	Resistance[Ω]	0.23
$8\Delta C$	Capacitance [nF]	3.9
	Resistance[Ω]	0.05
$16\Delta C$	Capacitance [nF]	8.0
	Resistance[Ω]	0.07

that the output voltage reaches its maximum value when the capacitance is 36 nF. Fig. 9(d) shows the AC/AC efficiency. Fig. 9(d) shows that the efficiency is maximized by correcting the resonance misalignment. The overall low efficiency in Fig. 9(d) is thought to be due to the large ESR of the resonant capacitor such as C_0, C_{1s}, C_2. The above results in Fig. 9 show that the proposed method can compensate for resonance misalignment while controlling the power.

Next, Fig. 10(a), (b) show the waveforms of the voltage input to the LCC circuit, the current flowing through the Tx coil, the output current flowing through the S circuit on the Rx side, and the output voltage of the S circuit, respectively, without and with compensation for resonance shift. The band-pass characteristics of each side result in a clean sine wave. When the resonance misalignment is compensated, the phase difference between the Tx and Rx coil currents is close

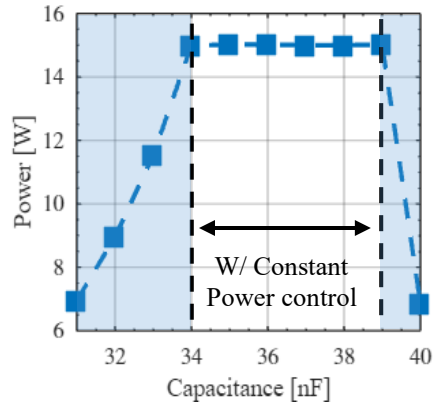

(a)

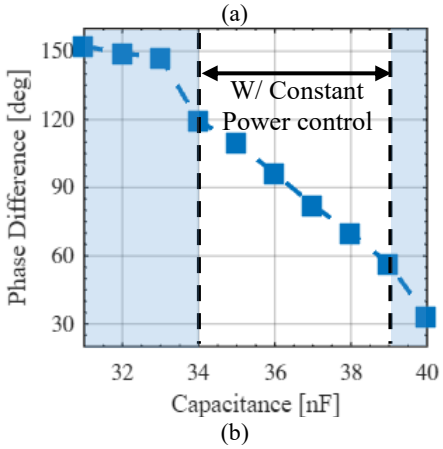

(b)

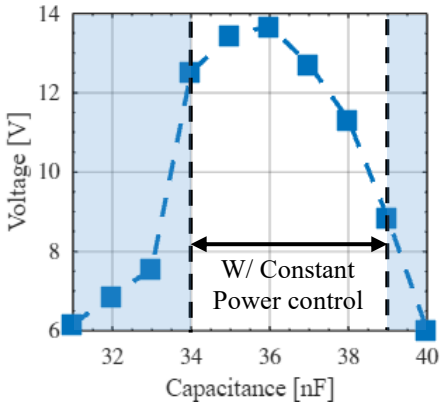

(c)

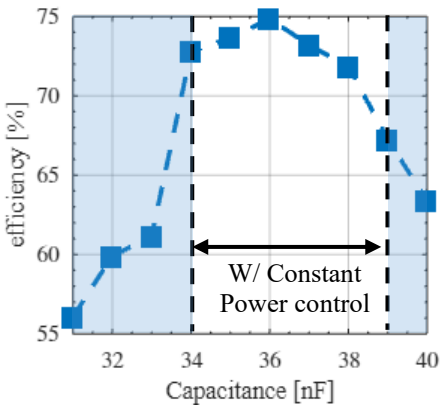

(d)

Fig. 9 Experimental results of steady-state performance according to C_2. (a) DC/DC converter output Power. (b) Phase difference between I_1 and I_2. (c) output AC voltage. (d) AC/AC efficiency.

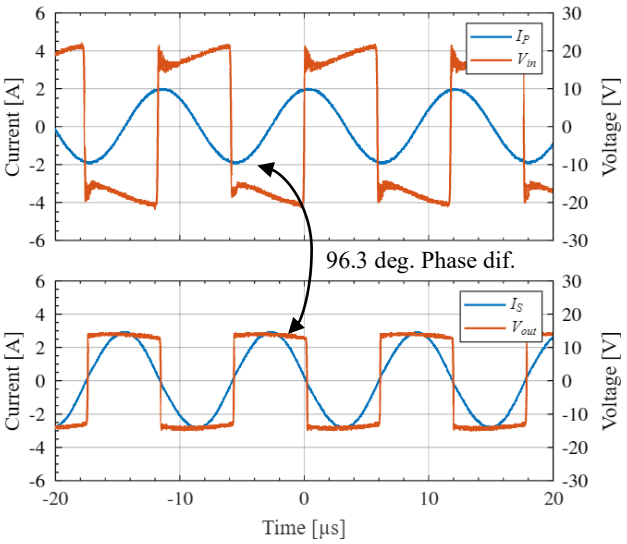

(a)

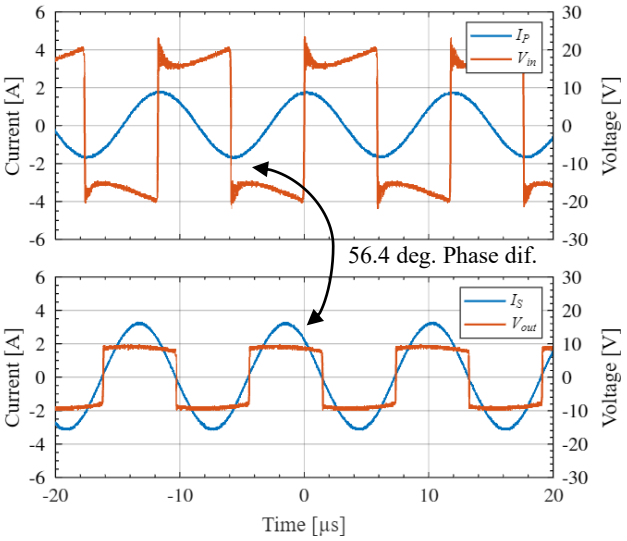

(b)

Fig. 10 Experimental waveform with/without MPT algorithm. (a)w/ MPT ($C_2 = 36$ nF). (b)w/o MPT ($C_2 = 39$ nF).

to 90°. The distortion of the LCC input voltage with and without resonance compensation is due to the voltage drop caused by the ESR of the lead wire from the inverter output to the voltage measurement point.

The above results are summarized in TABLE V. "w/ MPT" represents the transmission characteristics at 36 nF capacitance, when the voltage was at its maximum, and "w/o MPT" represents the result at 39 nF, when constant power is maintained but resonance misalignment is occurring. Comparing the results in TABLE V, it was found that the efficiency can be maximized by controlling C_2.From the above, it was found that by changing the capacitance and tracking the maximum voltage point, power control can be performed concurrently with resonance misalignment compensation.

TABLE V. PAFPRMANCE COMPARISON.

	P_{DC}	η	Phase
W/ MPT ($C_2 = 36$ nF)	15.0 [W]	74.9 %	96.3 deg
W/o MPT ($C_2 = 39$ nF)	15.0 [W]	67.3 %	56.4 deg

V. CONCLUSION

This paper proposes a method of compensating for resonance misalignment in WPT using a branched capacitor. The principle of the proposed control method is explained in the steady state of a WPT circuit. In this system, resonance misalignment compensation can be automatically performed only on the Rx side by maximizing the voltage output of the S circuit on the Rx side. The proposed method does not require communication between Tx and Rx or resonance misalignment compensation on the Tx side. The theory is verified by simulation and experimental measurement results of static characteristics. Each result shows that it is possible to compensate for resonance misalignment while protecting the system from excessive power with a DC/DC converter.

Future works include the three following issues. First, automatic adjustment of the variable capacitor has not been conducted experimentally, only by simulation in this paper. Therefore, it is necessary to implement the variable capacitor such as [18]-[21] and conduct experiments on automatic adjustment. Second, in practical WPT systems, batteries are often connected behind the rectifier. Therefore, it is necessary to study the control method when a constant voltage load is connected instead of a resistive load. Third, hard switching of the inverter should be considered. Resonance misalignment causes the input impedance of the WPT circuit to become capacitive, and hard switching causes a reduction in DC/DC efficiency[20]. As a future work, it is necessary to consider a system that can achieve soft switching even when resonance misalignment occurs.

REFERENCES

[1] G G. A. Covic and J. T. Boys, “Inductive power transfer,” Proc. IEEE, vol. 101, no. 6, pp. 1276–1289, Jun. 2013.

[2] Y. Yamada, T. Imura and Y. Hori, "Theorizing a Simple Ferrite Cored Coil Using Image Coils in Wireless Power Transfer," in IEEE Access, vol. 11, pp. 8065-8072, 2023.

[3] Y. Yamada and T. Imura, “An Efficiency Optimization Method of Static Wireless Power Transfer Coreless Coils for Electric Vehicles in the 85 kHz Band Using Numerical Analysis,” IEEJ Trans. Electr. Electron. Eng., vol. 17, no. 10, pp. 1506–1516, Oct. 2022.

[4] S. Urano, M. Sugizaki, T. Imura and Y. Hori, "Basic Experiment on the Integration of Grid-Connected Photovoltaic and Dynamic Wireless Power Transfer," 2022 IEEE 7th Southern Power Electronics Conference (SPEC), Nadi, Fiji, 2022, pp. 1-6.

[5] K. Yokoi, Y. Yasuda, A. Kanbe, T. Imura, and S. Aoki, “Development of Wireless Power-Transmission-Based Photodynamic Therapy for the Induction of Cell Death in Cancer Cells by Cyclometalated Iridium(III) Complexes,” Molecules, vol. 28, no. 3, p. 1433, Feb. 2023.

[6] S. Lee et al., "Voltage-Boosted Current-Mode Wireless Power Receiver for Directly Charging a Low-Voltage Battery in Implantable Medical Systems," in IEEE Transactions on Industrial Electronics, vol. 66, no. 11, pp. 8860-8865, Nov. 2019.

[7] S. Honda et al., "Proposal and Evaluation of High-Heat Insulation System for Spacecraft by Using WPT", IEEJ Journal of Industry Applications, vol.12, No.3, pp. 467-474, May. 2023.

[8] T. Imura and Y. Hori, "Unified Theory of Electromagnetic Induction and Magnetic Resonant Coupling", IEEJ Transactions on Industry Applications, Vol.135, No.6, pp. 697-O6710, June. 2015. (in Japanese)

[9] S. Y. Jeong, J. H. Park, G. P. Hong and C. T. Rim, "Autotuning Control System by Variation of Self-Inductance for Dynamic Wireless EV Charging With Small Air Gap," in IEEE Transactions on Power Electronics, vol. 34, no. 6, pp. 5165-5174, June 2019.

[10] Y. Zhang, T. Kan, Z. Yan and C. C. Mi, "Frequency and Voltage Tuning of Series–Series Compensated Wireless Power Transfer System to Sustain Rated Power Under Various Conditions," in IEEE Journal of Emerging and Selected Topics in Power Electronics, vol. 7, no. 2, pp. 1311-1317, June 2019.

[11] K. Lu, Y. Wang, Y. Yao, Y. Guan and D. Xu, "A Novel WPT System with Digitally Closed-loop Control Featuring High Misalignment Tolerance," 2019 IEEE 4th International Future Energy Electronics Conference (IFEEC), Singapore, 2019, pp. 1-6.

[12] Z. Liu, L. Wang, C. Yin, Y. Guo and C. Tao, "A Research on Constant Voltage Output Characteristics of Wireless Power Transfer System with A DC-DC Converter," 2019 IEEE 15th Brazilian Power Electronics Conference and 5th IEEE Southern Power Electronics Conference (COBEP/SPEC), Santos, Brazil, 2019, pp. 1-4.

[13] A. K. Yadav, A. Sankar and A. Khaligh, "A Three Stage Architecture for a High Voltage Step-Down Wireless Charging System," 2020 IEEE Energy Conversion Congress and Exposition (ECCE), Detroit, MI, USA, 2020, pp. 1002-1007.

[14] H. Weerasekara, K. Hata, T. Imura, H. Fujimoto and Y. Hori, "Efficiency Maximization in Wireless Power Transfer Systems for Resonance Frequency Mismatch," 2019 IEEE PELS Workshop on Emerging Technologies: Wireless Power Transfer (WoW), London, UK, 2019, pp. 363-366.

[15] K. Song et al., "An Impedance Decoupling-Based Tuning Scheme for Wireless Power Transfer System Under Dual-Side Capacitance Drift," in IEEE Transactions on Power Electronics, vol. 36, no. 7, pp. 7526-7536, July 2021.

[16] Y. Luo, Y. Yang, S. Zhang, X. Luo and L. Li, "Performance Analysis and Optimization of The MCR-WPT System with Uncertain Parameters," 2020 IEEE Wireless Power Transfer Conference (WPTC), 2020, pp. 154-158.

[17] W. Li, Q. Zhang, C. Cui and G. Wei, "A Self-Tuning S/S Compensation WPT System Without Parameter Recognition," in IEEE Transactions on Industrial Electronics, vol. 69, no. 7, pp. 6741-6750, July 2022.

[18] S. A. Chowdhury, S. -W. Kim, S. -M. Kim, J. Moon, I. -K. Cho and D. Ahn, "Automatic Tuning Receiver for Improved Efficiency and EMI Suppression in Spread-Spectrum Wireless Power Transfer," in IEEE Transactions on Industrial Electronics, vol. 70, no. 1, pp. 352-363, Jan. 2023.

[19] R. Matsumoto and H. Fujimoto, "Adaptive Compensation Scheme for Wireless Power Transfer Systems with Coil Inductance Variation Using PWM-Controlled Switched Capacitor," 2022 Wireless Power Week (WPW), Bordeaux, France, 2022, pp. 244-248.

[20] R. Matsumoto, T. Fujita and H. Fujimoto, "Communication-Less Reactance Compensation Using PWM-Controlled Switched Capacitors for Wireless Power Transfer," in IEEE Transactions on Power Electronics, to be published, doi: 10.1109/TPEL.2023.3294487.

[21] R. Matsumoto and H. Fujimoto, "Wireless EV Charging System Using PWM-Controlled variable Capacitor for Maximum Power Transfer under Severe Coil Misalignment," 2022 International Power Electronics Conference (IPEC-Himeji 2022- ECCE Asia), 2022.

[22] K. Matsuura, D. Kobuchi, Y. Narusue and H. Morikawa, "Communication-Less Receiver-Side Resonant Frequency Tuning for Magnetically Coupled Wireless Power Transfer Systems," in IEEE Access, vol. 11, pp. 23544-23556, 2023